Earthquakes and Structures, *Vol. 17, No. 3* (*2019*) *307-315*
DOI: https://doi.org/10.12989/eas.2019.17.3.307

Prediction and control of buildings with sensor actuators of fuzzy EB algorithm

Tim Chen[1a], Alex Bird[2], John Mazhar Muḥammad[3], S. Bhaskara Cao[4], Charles Melvilled[4] and C.Y.J. Cheng[*5]

[1]*AI LAB, Faculty of Information Technology, Ton Duc Thang University, Ho Chi Minh City, Vietnam*
[2]*National Physical Laboratory, New Delhi, Dr KS Krishnan Marg, Pusa, New Delhi, Delhi 110012, India*
[3]*Computer Simulation Research Laboratory, University of Oxford, Parks Road, Oxford, OX1 3PJ UK*
[4]*National University of Sciences and Technology (NUST), School of Natural Sciences, H-12, Islamabad*
[5]*Department of Automatic Control, University of Southern Queensland, Darling Heights, TOOWOOMBA QLD 4350, Australia*

(*Received August 15, 2018, Revised July 11, 2019, Accepted July 15, 2019*)

Abstract. Building prediction and control theory have been drawing the attention of many scientists over the past few years because design and control efficiency consumes the most financial and energy. In the literature, many methods have been proposed to achieve this goal by trying different control theorems, but all of these methods face some problems in correctly solving the problem. The Evolutionary Bat (EB) Algorithm is one of the recently introduced optimization methods and providing researchers to solve different types of optimization problems. This paper applies EB to the optimization of building control design. The optimized parameter is the input to the fuzzy controller, which gives the status response as an output, which in turn changes the state of the associated actuator. The novel control criterion for guarantee of the stability of the system is also derived for the demonstration in the analysis. This systematic and simplified controller design approach is the contribution for solving complex dynamic engineering system subjected to external disturbances. The experimental results show that the method achieves effective results in the design of closed-loop system. Therefore, by establishing the stability of the closed-loop system, the behavior of the closed-loop building system can be precisely predicted and stabilized.

Keywords: intelligent control; system design; fuzzy theory; bat algorithm; fuzzy optimization

1. Introduction

In the past two decades, a large number of studies have been carried out on the development and implementation of active, semi-active and hybrid control of structures (e.g., Connor 2003, Adeli 2004, Kim and Adeli 2004, Adeli and Jiang 2006, Jiang and Adeli 2005), and various control strategies such as sliding mode control have been proposed. However, most of the research has focused on the application of classical linear control theory, such as linear quadratic regulator (LQR) feedback control algorithm and linear quadratic Gaussian (LQG) control algorithm. In order to implement the LQR regulator, we must be able to measure all states of the system. This is obviously an unrealistic assumption, and we can only measure the sensor output. All sensors have noise, which means our measurements are not perfect. In addition, real systems always have some type of interference or process noise that affects them, which destroys the state equation. Therefore, we need a way to reconstruct our equations of state and generate their estimates, using our noise measurements and considering the interference entering the factory. We will not delve into the details of probability theory in this article, but jump directly into the results. Readers interested in this topic can refer to the original paper by Kalman (1963).

These algorithms only effectively control the structural response when the structure is small and a linear behavior is assumed. In order to effectively design a system control theory for a building, an effective control system and standard is needed that can reduce total consumption without compromising the user's preferred deployment within the building. In the literature, many methods have been proposed to achieve this goal by trying different control theorems, but all of these methods face some problems in correctly solving the problem. The Evolutionary Bat Algorithm (EBA) is one of the recently introduced optimization methods and has attracted the attention of researchers to solve different types of optimization problems. This paper applies EBA to the optimization of building control design, which is one of the most interesting optimization problems in recent years. The optimized parameter is the input to the fuzzy controller, which gives the status response as an output, which in turn changes the state of the associated actuator.

In recent years, fuzzy logic control (FLC) has been used in many successful real-world control applications since the success of the presentation in Zadeh (1965) (Kickert and Mamdani 1978, Braae and Rutherford 1979, Chang and Zadeh 1972, Buvana and Jayashree 2019). Despite the success, it is clear that many basic issues remain to be resolved. In this paper, the Takagi-Sugeno (T-S) fuzzy dynamic model consists of fuzzy IF-THEN rules (Takagi and Sugeno 1985), which represent the local linear input-

*Corresponding author, Ph.D.
E-mail: jc343965@gmail.com
[a]Ph.D.
E-mail: timchen@tdtu.edu.vn

http://www.techno-press.com/journals/eas&subpage=7 ISSN: 2092-7614 (Print), 2092-7622 (Online)

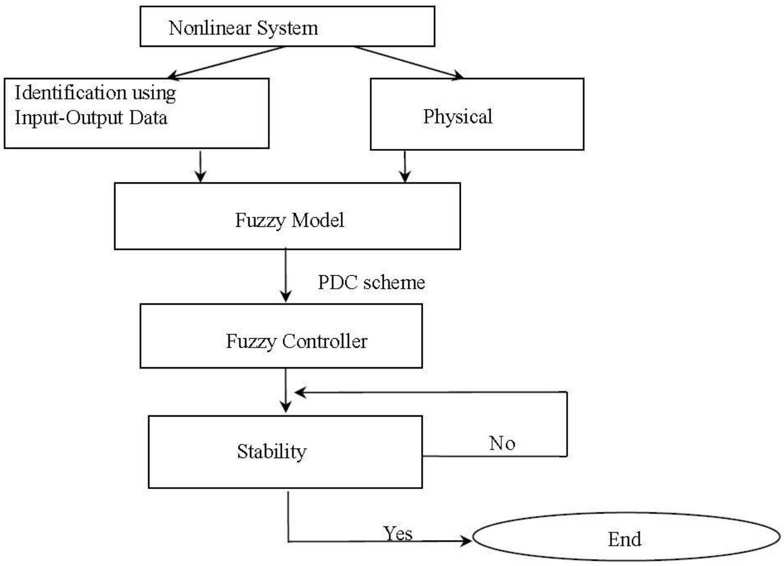

Fig. 1 Introduction the complete design procedure

output relationship of systems. This simple and versatile modeling approach attempts to express each fuzzy meaning through a linear system model. This allows us to use linear feedback control techniques with stable feedback. Wang *et al*. (1996) introduced the concept of a parallel distributed compensation (PDC) scheme. Used to design a fuzzy controller to stabilize the fuzzy model. Our idea is to design a compensator for each rule of the fuzzy model. Since each control rule is designed separately according to the corresponding rules of the T-S fuzzy model, the linear control design technique can be used to design the PDC fuzzy controller. The resulting overall fuzzy controller is typically non-linear and is a fuzzy blend of each individual linear controller. The fuzzy controller of each rule shares the same fuzzy set as the fuzzy model in the premise section.

In addition, intelligence is also a popular area that has caught the attention of many researchers. Many algorithms are inspired by the wisdom of creatures in nature, and these algorithms are included in this field. In general, swarm intelligence methods require evolutionary computation and mimic the specific behavior or survival skills of the creature. For example, Tsai *et al*. (2012) presented the bat-based prey discovery process proposes the Evolutionary Bat Algorithm (EBA). The algorithms have been applied to solve many problems in engineering. In this paper, the EBA is applied to the optimization of control design of buildings, which is one of the most concerned optimization problems in recent years. The optimized parameters are the input to the fuzzy controller, which gives response of states as an output, which in turn changes the state of the associated actuator. The closed-loop building system's behavior can be rigorously predicted and controlled by establishing the controller design procedure closed-loop fuzzy system in Fig. 1.

2. Composite structure problems and motion systems

Assume that the equation of motion for a shear-type-building modeled by an n-degrees-of-freedom system controlled by actuators and subjected to ground excitation can be written as follows

$$M\ddot{\bar{X}}(t) + C\dot{\bar{X}}(t) + K\bar{X}(t) = \bar{B}U(t) - M\bar{r}\ddot{x}_g \tag{1}$$

where $\bar{X} = [\bar{x}_1, \bar{x}_2, \cdots \bar{x}_n]^T \in R^n$ is an n-vector denoting the interfloor drift of the designated ith story unit. Matrices *M*, *C* and *K* are n×n mass, damping and stiffness matrices, respectively. The m-dimensional control force vector *U*(*t*) corresponds to the actuator forces (generated via active tendon system or an active mass damper, for example); this is only a static model, neglecting the dynamic equations of actuators. A discussion of their dynamic delay effects is given in the following section.

For controller design, the standard first-order state equation corresponding to Eq. (1) is

$$\dot{X}(t) = AX(t) + BU(t) + E\ddot{x}_g \tag{2}$$

where $X^T = [\bar{X}^T \quad \dot{\bar{X}}^T]$ is a 2*n* vector and

$$A = \begin{bmatrix} 0 & I_{n\times n} \\ -M^{-1}K & -M^{-1}C \end{bmatrix} \quad B = \begin{bmatrix} 0 \\ M^{-1}\bar{B} \end{bmatrix} \quad E = \begin{bmatrix} 0 \\ -\bar{r} \end{bmatrix}.$$

We have come to the LQ regularity, which lacks the assumption that all states are available for measurement, and we have also developed a Kalman filter that produces the best estimate of the state in the sense of equation. We can put them together and use a minimum standard control law (Athans *et al*. 1986). A so-called linear quadratic Gaussian or LQG optimal controller is obtained. The solution to the LQG problem is defined by the separation principle, which states that the best results are achieved by using the following procedure. First, the best estimate of state X(t) is obtained, and then the estimate is used as if it were an accurate measure of the state to solve the deterministic LQ control problem. Since both the LQ regulator and the Kalman filter are robust, it is expected that the LQG optimal controller will generally produce good robustness. Doyle and Stein (1981) has demonstrated that the LQG optimal controller can exhibit an arbitrarily poor stability margin. A fundamental limitation of LQG to structural control is the lack of robustness; that is, if the modeled plant dynamics of the model are different from the actual plant dynamics (only slightly), then predicted on the wrong model when finally interconnected with the structure. LQG designs can create unstable closed loop systems.

LQG/LTR is an elegant method for achieving the required system performance and maximum robustness in the design of feedback control systems (Doyle and Stein 1981, Stein and Athans 1987). In a sense, it is an integrated process that uses frequency and time domain concepts. Performance and robustness requirements are specified in the frequency domain, while most calculations are done in the time domain. The solution program basically involves a two-step approach. First, design a Kalman filter with the required loop transmission characteristics. Then a series of LQ feedback regulators close to the ideal limit are designed, which makes the stability margin asymptotically close to the stability margin of the Kalman filter. This method is easy to implement because it mainly involves repeated solutions of the algebraic Riccati equation.

The first step of the design process is to shape the singular values of the so-called target feedback loop (TFL) in the frequency domain. The Kalman Filter methodology can be applied to the TFL design. Consider the fictitious stochastic state dynamics

$$\begin{aligned} \dot{X}_a(t) &= A_a X(t) + B_a U(t) + \Gamma \varepsilon(t) \\ Y(t) &= C_a X(t) + n(t) \end{aligned} \tag{3}$$

where fictitious process noise $\varepsilon(t)$ is white, zero mean, with unity intensity matrix, and the measurement noise $n(t)$ is white, zero mean, and with intensity matrix equal to μI. The solution to the Kalman Filter problem yields the formula for calculating the filter gain matrix $L = (1/\mu)P_f C_a^T$ and P_f is the constant, symmetric, positive semidefinite matrix which is the solution to filter algebraic Riccati equation

$$A_a P_f + P_f A_a^T + \Gamma\Gamma^T - (1/\mu) P_f C_a^T C_A P_f = 0 \tag{4}$$

A distinction must be noted in this procedure; the Kalman filter formula and concepts are used as a means to an end, rather than in a precise optimal stochastic estimation and control context. The second and final step of the LQG/LTR design process involves the "recovery" of the TFL transfer matrix $G_{TFL}(s)$ by the compensated plant transfer matrix $G_a(s)K_{LQG/LIR}(s)$. The LQG/LTR method allows us to find $K_{LQG/LIR}(s)$ so that there is an approximate relation $G_a(s)K_{LQG/LIR}(s) \approx G_{TFL}(s)$ over the band of frequencies relevant to our concerns for robustness and performance. The *LQG/LTR* controller belongs to the class of so-called model-based controllers. One feedback loop involves the filter gain matrix L and the other loop involves controlling the gain matrix F. The filter gain L is fixed to be found in the *TFL*, as discussed in the first design step. The only remaining design gain matrix in $K(s)$, the control gain matrix F, is calculated by a solution called the Low Cost Control Linear Quadratic Regulator (*LQR*) problem, as described below.

Let the state weighting Q_c and the control weighting R_c be chosen as $Q_C = C_a{}^T C_a$, $R_C = \rho I$ where ρ is the recovery parameter. To compute the control gain matrix F for the *LQG/LTR* controller, we solve the algebraic Riccati equation

$$P_\rho A_a + A_a^T P_\rho + C_a^T C_a - (1/\rho) P_\rho B_a B_a^T P_\rho = 0 \tag{5}$$

The presence of a general performance limit (Maciejowski 1989) within the right half of the system's required bandwidth is not considered a charge for the method.

The structural model order reduction problem can generally be said as follows: Given a complete order structure model $G(s)$, find a low-order model, such as an rth order model, so that $G(s)$ is close in some sense. In this report, we hope that the reduced structural model is like

$$G(s) = \hat{G}_r(s) + \tilde{\Delta}_a(s) \tag{6}$$

and the additive modeling error is small in infinity norm.

The state space truncation method removes unimportant states from the state space model. Without loss of generality, let us ignore the effects of earthquake excitation and consider the full-order structural model G(s) given by

$$\begin{aligned} \dot{X}(t) &= AX(t) + BU(t) \\ Y(t) &= CX(t) + DU(t) \end{aligned} \tag{7}$$

Divide the state vector X into components to be retained and components to be discarded

$$X(t) = \begin{bmatrix} X_1(t) \\ X_2(t) \end{bmatrix}. \tag{8}$$

The r-vector contains the components to be retained, while the $(n\text{-}r)$-vector contains the components to be discarded. Now partition the matrices A, B and C conformably with X to obtain

$$A = \begin{bmatrix} A_{11} & A_{12} \\ A_{21} & A_{22} \end{bmatrix}, \quad B = \begin{bmatrix} B_1 \\ B_2 \end{bmatrix}, \quad C = \begin{bmatrix} C_1 & C_2 \end{bmatrix}. \tag{9}$$

If $X_2(t)$ represents the fast dynamics of the system, we may approximate the low-frequency behavior by setting $\dot{X}_2(t)$=0. This gives the quasi-steady-state solution (Lu *et al*. 1998)

$$X_2(t) = -A_{22}^{-1}(A_{21}X_1(t) + B_{22}U(t)) \tag{10}$$

provided A_{22}^{-1} is nonsingular.

Eliminating $X_2(t)$ from Eq. (7) yields

$$\begin{aligned} \dot{X}_1(t) &= (A_{11} - A_{12}A_{22}^{-1}A_{21})X_1(t) + (B_1 - A_{12}A_{22}^{-1}B_2)U(t) \equiv \hat{A}_{11}X_1(t) + \hat{B}_1 U(t) \\ Y(t) &= (C_1 - C_2 A_{22}^{-1}A_{21})X_1(t) + (D - C_2 A_{22}^{-1}B_2)U(t) \equiv \hat{C}_1 X_1(t) + \hat{D}U(t). \end{aligned} \tag{11}$$

The rth-order reduced model given by state-space truncation method is

$$\hat{G}_r(s) \equiv T_r(A,B,C,D) \equiv (\hat{A}_{11}, \hat{B}_1, \hat{C}_1, \hat{D}) = \hat{C}_1(sI - \hat{A}_{11})^{-1}\hat{B}_1 + \hat{D} \tag{12}$$

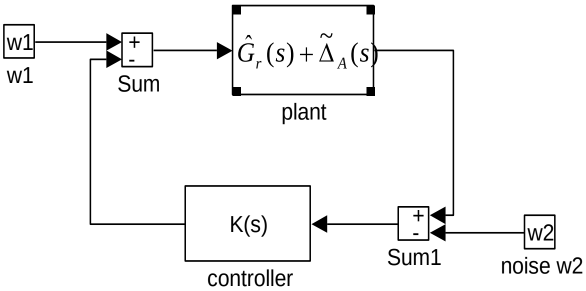

Fig. 2 Uncertainty representations for the active structural control system

The state-space truncation is a simple but general procedure for generating reduced-order models. Because $G(s)$ can have an infinite number of state-space realization by means of nonsingular transformation, there are, in principle, an infinite number of candidate truncation schemes. The property of the reduced-order model depends on the realization selected for truncation; for a truncation scheme to be useful, it must preserve stability and carry it with a guaranteed error bound.

Although there are an infinite number of different state space implementations for a given model $G(s)$, the analysis of the degree of participation in states in the energy transfer from past inputs to future outputs drives the consideration of balanced implementation as an appropriate implementation.

Consider the LQ (Linear Quadratic) problem

$$\min_{u\in L_2(-\infty,0]} \int_{-\infty}^{0} U^T(t)U(t)dt \tag{13}$$

subject to

$$\dot{X}_b = A_b X_b + B_b U(t) \tag{14}$$

with

$$X_b(0) = X_{0b} \tag{15}$$

From the result of Moore (1981), we can conclude that

$$\max_{u\in L_2(-\infty,0];X(0)=X_{0b}} \frac{\int_0^{\infty} Y^T(t)Y(t)dt}{\int_{-\infty}^{0} U^T(t)U(t)dt} = \frac{X_{0b}^T Q X_{0b}}{X_{0b}^T P^{-1} X_{0b}} = \frac{X_{0b}^T \Sigma X_{0b}}{X_{0b}^T \Sigma^{-1} X_{0b}} = \sum_{i=1}^{n} \sigma_i^2 x_{0b_i}^T x_{0b_i} \tag{16}$$

Model reduction by balanced truncation simply applies the truncation operation to a balanced realization of a full-order model $G(s)$. Furthermore, it satisfies the twice-the -sum-of-the-tail infinity norm bound (Enns 1984)

$$\left\|\tilde{\Delta}_a(s)\right\|_\infty \equiv \left\|G(s) - \hat{G}_r(s)\right\|_\infty \le 2(\sigma_{r+1} + \sigma_{r+2} + \ldots + \sigma_n) \tag{17}$$

where the infinity norm is defined as

$$\left\|\tilde{\Delta}_a(s)\right\|_\infty \equiv \sup_\omega \bar{\sigma}[\tilde{\Delta}_a(j\omega)] \tag{18}$$

Recall that singular values of matrix A are the square roots of the eignvalues of A^*A; i.e.

$$\sigma_i^2(A) = \lambda_i(A^*A) \tag{19}$$

where A^* is the complex conjugate transpose of A (Maciejowski 1989). And $\bar{\sigma}(A)$ and $\underline{\sigma}(A)$ denote the maximum and minimum singular value of A respectively.

The following lemma and definition quantify the tolerable size of $\tilde{\Delta}_a(s)$ in terms of singular value of $\hat{G}_r(s)$ and establish a relationship with the achievable control-loop bandwidth.

The following lemma and definition quantify the tolerable size of $\tilde{\Delta}_a(s)$ in terms of singular value of $\hat{G}_r(s)$ and establish a relationship with the achievable control-loop bandwidth.

Lemma 1: Consider the system shown in the Fig. 2. Suppose that $\tilde{\Delta}_a(s)$ has no unstable poles and that the controller stabilizes the reduced order structural model $\hat{G}_r(s)$. If for all frequency ω

$$\frac{\bar{\sigma}(\tilde{\Delta}_a(j\omega))}{\underline{\sigma}(\hat{G}_r(j\omega))}\bar{\sigma}[\hat{G}_r(j\omega)K(j\omega)(I+\hat{G}_r(j\omega)K(j\omega))^{-1}] < 1 \tag{20}$$

then controller K stabilizes the full order structural model $G(s)$. Given $G(s)$, $\hat{G}_r(s)$ and $\tilde{\Delta}_a(s)$ as defined earlier, the robust frequency is

$$\omega_r \equiv \max\{\omega | \underline{\sigma}(\hat{G}_r(j\omega)) \ge \bar{\sigma}(\tilde{\Delta}_a(j\omega))\} \tag{21}$$

Loosely speaking, the bandwidth of a control system is the frequency range where the open-loop transfer function is large, i.e.

$$\underline{\sigma}(\hat{G}_r(j\omega)K(j\omega)) >> 1 \tag{22}$$

for all

$$\omega < \omega_B \tag{23}$$

Notice (23) implies

$$\bar{\sigma}\{\hat{G}_r(j\omega)K(j\omega)[I+\hat{G}_r(j\omega)K(j\omega)]^{-1}\} \approx 1 \tag{24}$$

and

$$\underline{\sigma}(\hat{G}_r(j\omega)) > \bar{\sigma}(\tilde{\Delta}_a(j\omega)) \tag{25}$$

The significance of the robust frequency in the context of model reduction is that the frequency is an upper bound on the bandwidth ωB of any control system whose controller is designed on the reduced order model $\hat{G}_r(s)$.

Fig. 3 shows the closed-loop configuration of the feedback control system with the controller $K(s)$ to be designed on the reduced-order model. From Fig. 3 the following equation can be derived

$$\begin{aligned} Y(s) &= \hat{G}_r(s)K(s)[I+\hat{G}_r(s)K(s)]^{-1} \\ &[r(s)-n(s)] + [I+\hat{G}_r(s)K(s)]^{-1} d(s) \end{aligned} \tag{26}$$

For controller design, the additive model error can be considered as high frequency modeling uncertainty, and the effect of can be ignored from the preliminary controller design. This performance consideration must be tempered with a bandwidth limitation so that high frequency unmolded dynamics do not cause system instability, while the decision of system bandwidth is usually based on the

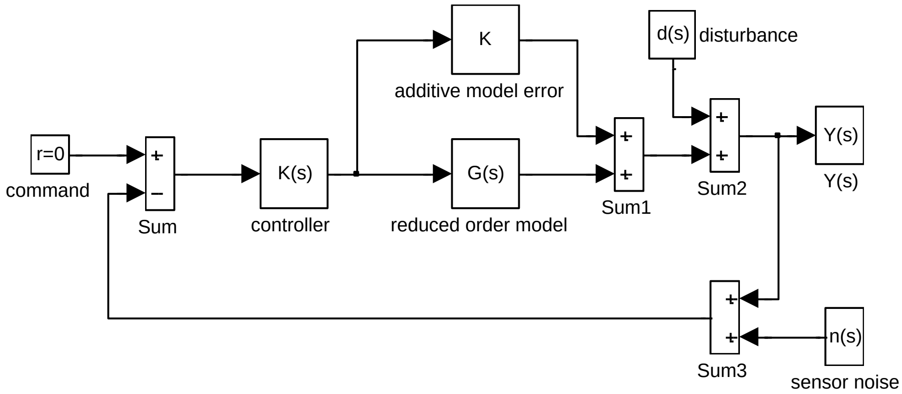

Fig. 3 The closed-loop configuration of the feedback control system

hard constrain: and some engineering judgments. In order to improve the low frequency performance of the feedback control system, the plant can augment with integrator one in each control channel before the LQG/LTR controller is to be designed. The overall outer-loop controller is

$$\mathrm{K(s)} = (\mathrm{I}/\mathrm{s})\mathrm{K}_{\mathrm{LQG/LTR}}(\mathrm{s}) \tag{27}$$

Define

$$\mathrm{G_a(s)} = \hat{\mathrm{G}}_\mathrm{r}(\mathrm{s})(\mathrm{I}/\mathrm{s}) \tag{28}$$

to be the augmented system consisting of reduced-order model and the integrator one in each control channel. The state-space representation of can be written as

$$\dot{X}_a = A_a X_a(t) + B_a U_a(t) \tag{29}$$

$$Y(t) = C_a X_a(t) \tag{30}$$

$$\mathrm{G_a(s)} = \mathrm{C_a}(\mathrm{sI} - \mathrm{A_a})^{-1}\mathrm{B_a} \tag{31}$$

where

$$X_a^T = (\underbrace{x_1, \ldots, x_m}_{\text{integrator-states}}, \underbrace{x_{m+1}, \ldots, x_{m+r}}_{\text{reduced-model-states}}) \tag{32}$$

$$A_a = \begin{bmatrix} 0 & 0 \\ \hat{B}_{b_1} & \hat{A}_{b_{11}} \end{bmatrix}, \quad B_a = \begin{bmatrix} I \\ 0 \end{bmatrix}, \quad C_a = [\hat{D}_{b_1} \quad \hat{C}_{b_1}] \tag{33}$$

then the *LQG/LTR* design procedure can be followed to design the controller $K_{LQG/LTR}(s)$ for augmented system $G_a(s)$.

3. Intelligent control system

3.1 Modified system

Consider a system $N(0;0)$ described by the following equation (Gauthier *et al*. 1994, Kapitaniak *et al*. 1993)

$$\dot{x}(t) = f(x, u) \tag{34}$$

where $x(t)$ is the state vector, $u(t)$ is the input vector and f is a vector-valued function which satisfies those assumptions of general continuity and boundedness given in Steinberg and Kadushin (1973).

For the convenience of presenting the control system structure in this paper, the remainder of this section is divided into two parts. The Takagi-Sugeno fuzzy model of the system is established and the PDC technique is used to design a fuzzy controller, and a stability criterion is given to determine whether the closed-loop fuzzy system $F(C,0)$ is stable.

The closed-loop fuzzy system $F(C,0)$

$$\dot{x}(t) = \frac{\sum_{i=1}^{r}\sum_{j=1}^{r} w_i(x(t))w_j(x(t))\{A_i - B_iK_j\}x(t)}{\sum_{i=1}^{r}\sum_{j=1}^{r} w_i(x(t))w_j(x(t))} \tag{35}$$

Which be rewritten as

$$\dot{x}(t) = \frac{1}{W}\left[\sum_{i=1}^{r} w_i(x(t))w_i(x(t))\{A_i - B_iK_i\}x(t) + 2\sum_{i<j}^{r} w_i(x(t))w_j(x(t))G_{ij}x(t)\right] \tag{35}$$

For the convenience of the stability analysis, we assume that $Q=P^{-1}$ (is a common positive definite matrix) and we can further define $W_i=K_iQ$, so that for $Q>0$ we have $K_i=W_iQ^{-1}$. Hence, according to the Lyapunov approach, the following lemma is given to guarantee the asymptotic stability of $F(C,0)$.

Lemma 2 (Wang and Tanaka 1996) The closed-loop fuzzy system is asymptotically stable in the large via PDC if there exist a and, such that the following linear matrix inequality (LMI) conditions hold

$$QA_i^T + A_iQ - B_iW_i - W_i^TB_i^T < 0 \tag{36}$$

In the following, based on Lemma 2, we synthesize a fuzzy controller to stabilize the system. However, not every fuzzy controller can satisfy the stability criterion. This implies that there may be no fuzzy controller available to stabilize. Hence, the closed-loop fuzzy system is classified into two types.

1) Type 1:. If is a common positive definite matrix and the stability conditions in Lemma 2 are satisfied, then the fuzzy controller can stabilize.

2) Type 2:. If is not a common positive definite matrix or the stability conditions in Lemma 2 are not satisfied, then the fuzzy controller and the dither (as an auxiliary of the

fuzzy controller) are simultaneously introduced to asymptotically stabilize the system when the fuzzy controller cannot stabilize $F_2(C,0)$.

Therefore, in the remainder of this paper, attention is devoted to the stability analysis of $F_2(C,0)$.

3.2 Stability of fuzzy control

The *T-S* fuzzy model of the model $N_R(0;0)$ is established. Subsequently, a fuzzy controller is obtained via the PDC scheme.

The ith rule of the fuzzy model $F_R(0;0)$ is represented as follows:

Model Rule:

The ith rule of the fuzzy controller is given as follows:

Control Rule i:

IF $x_{R1}(t)$ is $M_{i1}^R(\alpha_m,\beta_m)$ and … and $x_{Rk}(t)$ is $M_{ik}^R(\alpha_m,\beta_m)$

THEN $u_R(t) = -K_i(\alpha_m,\beta_m)x_R(t)$, (37)

Thus, the overall fuzzy controller is

$$u_R(t) = -\frac{\sum_{i=1}^{r} w_i(x_R(t),\alpha_m,\beta_m)K_i(\alpha_m,\beta_m)x_R(t)}{\sum_{i=1}^{r} w_i(x_R(t),\alpha_m,\beta_m)} \tag{38}$$

The derive the closed-loop fuzzy system $F_R(0;0)$ as follows

$$\dot{x}_R(t) = \frac{\sum_{i=1}^{r}\sum_{j=1}^{r} w_i(x_R(t),\alpha_m,\beta_m)w_j(x_R(t),\alpha_m,\beta_m)\{A_i(\alpha_m,\beta_m) - B_i(\alpha_m,\beta_m)K_j(\alpha_m,\beta_m)\}x_R(t)}{\sum_{i=1}^{r}\sum_{j=1}^{r} w_i(x_R(t),\alpha_m,\beta_m)w_j(x_R(t),\alpha_m,\beta_m)} \tag{39}$$

From above discussion, we can infer that if the dither has a sufficiently large frequency and a proper membership function is chosen, the trajectory of the closed-loop fuzzy system and that of the closed-loop system would be made as close as desired (Zames and Shneydor 1976, 1977, Wang and Abed 1995). This enables a rigorous prediction of the stability of the closed-loop system by establishing that of the closed-loop fuzzy system.

4. Stability design and EBA fuzzy algorithm

Hereafter, we are concerned with the stability of the closed-loop fuzzy system $F_R(C;0)$ instead of discussing the stability of the closed-loop system $N(C,d)$. Hence, the stability criterion of $F_R(C;0)$ is presented in the following.

Theorem 1 The closed-loop fuzzy system is asymptotically stable in the large via PDC if there exist a $Q>0$ and $W_i(\alpha_m,\beta_m)$, $i=1,2,\ldots,r$ such that the following LMI conditions hold

$$QA_i^T(\alpha_m,\beta_m) + A_i(\alpha_m,\beta_m)Q - B_i(\alpha_m,\beta_m)W_i(\alpha_m,\beta_m) - W_i^T(\alpha_m,\beta_m)B_i^T(\alpha_m,\beta_m) < 0$$

$$QA_i^T(\alpha_m,\beta_m) + A_i(\alpha_m,\beta_m)Q + QA_j^T(\alpha_m,\beta_m) + A_j(\alpha_m,\beta_m)Q - B_i(\alpha_m,\beta_m)W_j(\alpha_m,\beta_m) - W_j^T(\alpha_m,\beta_m)B_i^T(\alpha_m,\beta_m) - B_j(\alpha_m,\beta_m)W_i(\alpha_m,\beta_m),$$

$$-W_i^T(\alpha_m,\beta_m)B_j^T(\alpha_m,\beta_m) < 0 \tag{40}$$

where

$$W_i(\alpha_m,\beta_m) = K_iQ \ , \ W_j(\alpha_m,\beta_m) = K_jQ .$$

The proof of the above theorem can be similarly derived by following the same procedure as that in the proof of Wang and Tanaka (1996) but being replaced by $A_i(\alpha_m,\beta_m)$, $A_j(\alpha_m,\beta_m)$, $W_i(\alpha_m,\beta_m)$ and $W_j(\alpha_m,\beta_m)$, respectively. This proof is lengthy, so it is not repeated here.

The complete design procedure can be summarized in the following algorithm.

Problem: Given a system, how can we synthesize a fuzzy controller and find an appropriate dither signal to stabilize the closed-loop system?

Correctly select the parameter results for the appropriate step size to move the human agent in the solution space. This means improving the accuracy of finding an approximate optimal solution and reducing the likelihood of falling into local optimum. In our experiments, the medium chosen was air, because air is the original medium of existence in the natural environment in which bats live. A brief review of the operation of the EBA is as follows:

Step 1: Construct the *T-S* fuzzy model of the system.

Step 2: Utilize the concept of PDC technique to design a fuzzy controller. Subsequently, adjust the feedback gains and verify the stability condition of the closed-loop fuzzy system $F(C;0)$ by means of Lemma 2.

Step 3: If the stability condition of Lemma 2 cannot be satisfied by regulating the feedback gains, a dither, as an auxiliary of the fuzzy controller, is injected into $N(0;0)$.

Step 4: Apply the method to build the corresponding model.

Step 5: Reconstruct the T-S fuzzy model of $N_R(0;0)$ and use the PDC scheme to deduce the fuzzy controller.

Step 6: Derive the closed-loop fuzzy system by substituting the fuzzy controllerinto the fuzzy model. Furthermore, adjust the parameters (α_m, β_m) of the dither to satisfy the stability criterion of Theorem 1 (Mossaheb, 1983).

Step 7: The artificial agents are spread into the solution space by randomly assigning coordinates to them.

Step 8: The artificial agents are moved according to Eqs. (41)-(42). A random number is generated and then it is checked whether it is greater than the fixed pulse emission rate. If the result is positive, the artificial agent is moved using the random walk process.

$$x_i^t = x_i^{t-1} + D \tag{41}$$

where x_i^t indicates the coordinate of the ith artificial agent at the tth iteration, x_i^{t-1} represents the coordinate of the ith artificial agent at the last iteration, and D is the moving distance that the artificial agent goes in this iteration.

$$D = \gamma \cdot \Delta T \tag{42}$$

where γ is a constant corresponding to the medium chosen in the experiment, and $\Delta T \in [-1,1]$ is a random number.

γ=0.17 is used in our experiment because the chosen medium is air.

$$x_i^{t_R} = \beta \cdot (x_{best} - x_i^t), \beta \in [0,1] \quad (43)$$

where β is a random number; x_{best} indicates the coordinate of the near best solution found so far throughout all artificial agents; and $x_i^{t_R}$ represents the new coordinates of the artificial agent after the operation of the random walk process.

Step 9: The fitness of the artificial agents is calculated by the user defined fitness function and updated to the stored near best solution.

Step 10: Check the termination condition to decide whether to return to step 8 or terminate the program and output a near optimal solution.

The fitness function used in the evaluation process is a set of user-defined criteria. In other words, the fitness function is a mathematical representation of the solution space, and the user wishes to solve the problem or obtain an optimal solution for this purpose. Therefore, the fitness function is designed in this paper to find the common symmetric positive definite matrix and the control force of the controller.

5. Experiment and simulation result

Consider a building (Yang *et al*. 1998) in which each story unit is constructed identically. This 76-story building is modeled as a vertical cantilever beam. The finite element model is constructed by treating the building portion between two adjacent floors as a classic beam element of uniform thickness, resulting in 76 translations and 76 rotational degrees of freedom. Then, all 76 rotational degrees of freedom were removed by static condensation. This results in 76 degrees of freedom, indicating the displacement of each floor in the lateral direction. The first five natural frequencies are 0.16, 0.765, 1.992, 3.790, and 6.395 Hz, respectively. The proportional damping matrix of a building with 76 lateral degrees of freedom is calculated by using the Rayleigh method to assume a 1% damping ratio for the first five modes. The model has a mass, damping and stiffness matrix called the “76 DOF model”. The equation of motion of the building equipped with an ATMD on the top floor can be expressed as

$$\mathbf{M}\ddot{\mathbf{x}} + \mathbf{C}\dot{\mathbf{x}} + \mathbf{K}\mathbf{x} + \mathbf{H}\mathrm{u} = \boldsymbol{\eta}\mathbf{W}, \quad \beta \in [0,1] \quad (44)$$

in which $\mathbf{x} = [x_1, x_2, ..., x_{76}, x_m]'$ is the displacement vector with x_i being the displacement of the ith floor and x_m being the relative displacement of the inertial mass of damper with respect to the top floor, and a prime indicates the transpose of a vector or a matrix. In Eq. (44), *M*, *C*, and *K* are (77×77) mass, damping and stiffness matrices, *u* is a scalar control force, *W* is the wind excitation vector with dimension 77, *H* is a control influence vector, and η is an excitation influence matrix.

The resulting state equation is given by

$$\dot{\mathbf{x}} = \mathbf{A}\mathbf{x} + \mathbf{B}\mathrm{u} + \mathbf{E}\mathbf{W} \quad (45)$$

in which $\mathbf{x} = [\bar{\mathbf{x}}', \dot{\bar{\mathbf{x}}}']'$ is the 48-dimensional state vector and $\bar{\mathbf{X}} =$ [x_3, x_6, x_{10}, x_{13}, x_{16}, x_{20}, x_{23}, x_{26}, x_{30}, x_{33}, x_{36}, x_{40}, x_{43}, x_{46}, x_{50}, x_{53}, x_{56}, x_{60}, x_{63}, x_{66}, x_{70}, x_{73}, x_{76}, x_m]. In addition, A is a (48×48) system matrix, *B* is a (48×1) actuator location vector, and *E* is a (48×77) excitation influence matrix.

Similarly, the 76 DOF model (building without ATMD) can be reduced to a 23 DOF system by retaining the first 46 complex modes of the original system. The resulting state equation is also expressed by Eq. (44). In this case, however, the dimensions of *x*, *A*, *B*, and *E* are (46×1), (48×46), (48×1) and (48×76), respectively, and *u*=0. To further reduce the computational efforts, instead of reducing wind loads through the model reduction method (transformation) described above, the wind load vector W can be modelled physically by lumping wind forces on adjacent floors at the locations that correspond to the 24 DOF model (or 23 DOF model). Thus, in Eq. (44), the dimension of W becomes 24 and E is an appropriately modified (48×24) matrix. These simplified models are denoted by 24 DOF with W24 and 23 DOF with W23 models, respectively.

A nondimensionalized version of this performance criterion is given by

$$J_1 = \max\left\{\frac{\sigma_{\ddot{x}1}}{\sigma_{\ddot{x}75o}}, \frac{\sigma_{\ddot{x}30}}{\sigma_{\ddot{x}75o}}, \frac{\sigma_{\ddot{x}50}}{\sigma_{\ddot{x}75o}}, \frac{\sigma_{\ddot{x}55}}{\sigma_{\ddot{x}75o}}, \frac{\sigma_{\ddot{x}60}}{\sigma_{\ddot{x}75o}}, \frac{\sigma_{\ddot{x}65}}{\sigma_{\ddot{x}75o}}, \frac{\sigma_{\ddot{x}70}}{\sigma_{\ddot{x}75o}}, \frac{\sigma_{\ddot{x}75}}{\sigma_{\ddot{x}75o}}\right\} \quad (46)$$

where $\sigma_{\ddot{x}i}$ is the *rms* acceleration of the *i*th floor, and $\sigma_{\ddot{x}75o}$=9.914 cm/sec^2 is the rms acceleration of the 75th floor without control. In the performance criterion J_1, accelerations only up to 75th floor are considered because the 76th floor is the top of the building and it is not used by the occupants.

The second criterion is the average percentage of acceleration reduction for floors above the 49th floor, i.e.,

$$J_2 = \frac{1}{6}\sum_i [(\sigma_{\ddot{x}io} - \sigma_{\ddot{x}i})/\sigma_{\ddot{x}io}] \quad \text{for i= 50, 55, 60, 65,70 and 75} \quad (47)$$

in which $\sigma_{\ddot{x}io}$ is the *rms* acceleration of the *i*th floor without control. The third and fourth evaluation criteria are the ability of the controllers to reduce the floor displacements. The normalized version are given as follows

$$J_3 = \max\left\{\frac{\sigma_{x1}}{\sigma_{x76o}}, \frac{\sigma_{x30}}{\sigma_{x76o}}, \frac{\sigma_{x50}}{\sigma_{x76o}}, \frac{\sigma_{x55}}{\sigma_{x76o}}, \frac{\sigma_{x60}}{\sigma_{x76o}}, \frac{\sigma_{x65}}{\sigma_{x76o}}, \frac{\sigma_{x70}}{\sigma_{x76o}}, \frac{\sigma_{x75}}{\sigma_{x76o}}, \frac{\sigma_{x76}}{\sigma_{x76o}}\right\} \quad (48)$$

$$J_4 = \frac{1}{7}\sum_i [(\sigma_{xio} - \sigma_{xi})/\sigma_{xio}]; \quad (49)$$

for i= 50, 55, 60, 65,70, 75 and 76

where σ_{xi} and σ_{xio} are the *rms* displacements of the ith floor with and without control, respectively, and σ_{x76o}=10.040 cm is the rms displacement of the 76 floor of the uncontrolled building.

Each proposed control design must satisfy the actuator capacity constraints given by σ_u≤100 kN and σ_{xm}≤25 cm, where σ_u and σ_{xm} are rms control force and rms actuator stroke, respectively. In addition to above constraints, the control effort requirements of a proposed control design should be evaluated in terms of the following nondimensionalized criteria

$$J_5 = \sigma_{xm} / \sigma_{x76o} \tag{50}$$

$$J_6 = \sigma_{\dot{x}m} / \sigma_{\dot{x}76o} \tag{51}$$

in which $\sigma_{\dot{x}m}$ is the rms actuator velocity (relative velocity between the ATMD and the top floor). The performance criteria correspond to the physical size (i.e., stroke) and control power (i.e., actuator velocity) of the actuator. For the building without control, $\sigma_{\dot{x}76o}$ is 9.328 cm/sec.in which $\sigma_{\dot{x}m}$ is the rms actuator velocity (relative velocity between the ATMD and the top floor).

A numerical simulation (integration) for the on-line implementation of the proposed control design should be conducted to evaluate the performance in terms of the following non-dimensionalized criteria

$$J_7 = \max\left\{ \frac{\ddot{x}_{p1}}{\ddot{x}_{p75o}}, \frac{\ddot{x}_{p30}}{\ddot{x}_{p75o}}, \frac{\ddot{x}_{p50}}{\ddot{x}_{p75o}}, \frac{\ddot{x}_{p55}}{\ddot{x}_{p75o}}, \frac{\ddot{x}_{p60}}{\ddot{x}_{p75o}}, \frac{\ddot{x}_{p65}}{\ddot{x}_{p75o}}, \frac{\ddot{x}_{p70}}{\ddot{x}_{p75o}}, \frac{\ddot{x}_{p75}}{\ddot{x}_{p75o}} \right\} \tag{52}$$

$$J_8 = \frac{1}{6}\sum_i [(\ddot{x}_{pio} - \ddot{x}_{pi})/\ddot{x}_{pio}]; \quad \text{for } i\text{=50, 55, 60, 65,70 and 75} \tag{53}$$

$$J_9 = \max\left\{ \frac{x_{p1}}{x_{p76o}}, \frac{x_{p30}}{x_{p76o}}, \frac{x_{p50}}{x_{p76o}}, \frac{x_{p55}}{x_{p76o}}, \frac{x_{p60}}{x_{p76o}}, \frac{x_{p65}}{x_{p76o}}, \frac{x_{p70}}{x_{p76o}}, \frac{x_{p75}}{x_{p76o}}, \frac{x_{p76}}{x_{p76o}} \right\} \tag{54}$$

$$J_{10} = \frac{1}{7}\sum_i [(x_{pio} - x_{pi})/x_{pio}];$$

$$\text{for } i\text{=50, 55, 60, 65,70, 75 and 76} \tag{55}$$

where x_{pi}=peak displacement of ith floor, $\ddot{x}_{pi}$=peak acceleration of ith floor, x_{pio}=peak displacement of *i*th floor without control, and $\ddot{x}_{pio}$=peak acceleration of ith floor without control; for instance, x_{p76o}=26.009 cm and $\ddot{x}_{p75o}$= 26.334 cm/sec^2.

The actuator capacity constraints for the deterministic response analysis are: the maximum control force max|$u(t)$|≤300 kN and the maximum stroke max|$x_m(t)$|≤75 cm. In addition, the proposed control designs should be evaluated for the following control capacity criterion

$$J_{11} = x_{pm}/x_{p76o} \tag{56}$$

$$J_{12} = \dot{x}_{pm}/\dot{x}_{p76o} \tag{57}$$

where x_{pm}=peak stroke of actuator, $\dot{x}_{pm}$=peak velocity of the actuator, and $\dot{x}_{p75o}$=22.622 cm/sec=peak velocity of 76th floor without control.

However, the limitation is not applied for the controller gains because the total effect contributed to the whole system by the control force is relatively small. All parameters used in our experiment for EBA are listed in Table 1.

Like other swarm intelligence algorithms and evolution methods, EBA requires recursive operations to find the closest solution. Therefore, the same experiment should be repeated multiple times to test whether the convergence results are consistent. The number of runs listed in Table 1 is intended to provide a series of experimental results for examination by statistical methods. In this paper, we choose a fixed number of iterations as the termination criterion. The media material used to transmit the sound waves is chosen to be air because it is suitable for the natural environment in which the bat is located. In addition, the population size represents the number of human agents that exist simultaneously in the solution space in each iteration. The larger population size provides a greater opportunity for the algorithm to find the closest solution. However, a larger population size requires more memory resources and computing power. Therefore, we set the population size to 16 in the experiment. The number of feasible solutions that EBA obtains in different runs is shown in Fig. 4.

Table 1 Parameters for EBA

Boundary condition for matrix positive definite matrix and controller gains	[-5, 5]
Medium Material	Air
Number of Run	40
Population size	26
Number of Iteration	700

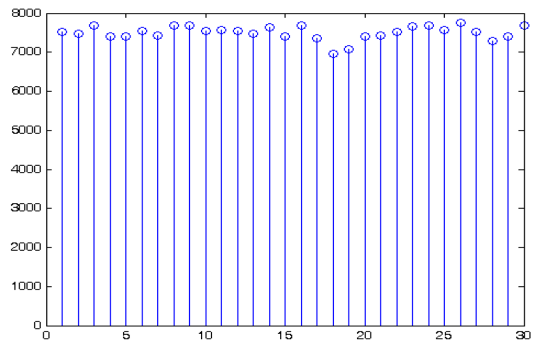

Fig. 4 Number of feasible solutions obtained by EBA in 40 runs

6. Conclusions

This article discusses the issue of optimizing controller design issues, in which the evolutionary bat optimization algorithm is combined with the fuzzy controller in the practical application of the building. The controller of the system design includes different sub-parts such as system initial condition parameters, EB optimal algorithm, fuzzy controller, stability analysis and sensor actuator. The advantage of the design is that if the controller is useless, the modified criterion of controller is derived by asymptotically adjusting design parameters. Numerical verification of the time domain and the frequency domain shows that the new system design provides accurate prediction and control of the structural displacement response, which is necessary for the active control structure in the fuzzy model. The dynamic fuzzy controller proposed in this paper is used to find the optimal control force required for active nonlinear control of building structures.

References

Adeli, H. and Jiang, X.M. (2006), "Dynamic fuzzy wavelet neural network model for structural system identification", *J. Struct. Eng.*, ASCE, **132**(1), 102-111. https://doi.org/10.1061/(ASCE)0733-9445(2006)132:1(102).

Adeli, H. and Kim, H. (2004), "Wavelet-hybrid feedback-least mean square algorithm for robust control of structures", *J. Struct. Eng.*, ASCE, **130**(2), 128-137. https://doi.org/10.1061/(ASCE)0733-9445(2004)130:1(128).

Athans, M., Kapasouris, P., Kappos, E. and Spang, H.A. (1986), "Linear quadratic gaussian with Loop-Transfer-Recovery Methodology for the F-100 engine", *J. Guid. Control Dyn.*, **9**(1), 45-51. https://doi.org/10.2514/3.20065.

Braae, M. and Rutherford, D.A. (1979), "Theoretical and linguistic aspects of the fuzzy logic controller", *Automatica*, **15**(5), 553-577. https://doi.org/10.1016/0005-1098(79)90005-0.

Buvana, D. and Jayashree, R. (2019), "ANFIS controller-based cascaded nonisolated bidirectional DC-DC converter", *J. Circuit. Syst. Comput.*, **28**(1), 1950001. https://doi.org/10.1142/S0218126619500014.

Chang, S.S.L. and Zadeh, L.A. (1972), "On fuzzy mapping and control", *Fuzzy Sets, Fuzzy Logic, Fuzzy Syst.*, Selected Papers by Lotfi A Zadeh, 180-184. https://doi.org/10.1142/9789814261302_0012.

Connor, J.J. (2003), *Introduction to Structural Motion Control*. Prentice-Hall, Upper Saddle River, NJ.

Doyle, J.C. and Stein, G. (1981), "Multivariable feedback design: concepts for classical/modern synthesis", *IEEE Tran. Auto. Control*, **26**(1), 4-16. https://doi.org/10.1109/TAC.1981.1102555.

Enns, D.F. (1984), "Model reduction with balanced realizations: An error bound and frequency weighted generalization", *Proc. 23rd Conference on Decision and Control*, Las Vegas.

Gauthier, D.J., Sukow, D.W., Concannon, H.M. and Socolar, J.E.S. (1994), "Stabilizing unstable periodic orbits in a fast diode resonator using continuous time-delay autosynchronization", *Phys. Rev. E.*, **50**, 2343-2346. https://doi.org/10.1103/PhysRevE.50.2343.

Jiang, X.M. and Adeli, H. (2005), "Dynamic wavelet neural network for nonlinear identification of highrise buildings", *Comput. Aid. Civil Infrastr. Eng.*, **20**(5), 316-330. https://doi.org/10.1111/j.1467-8667.2005.00399.x.

Kalman, R.E. (1963), "New methods in Wiener filtering theory", Eds. J.L. Bogdanoff and F. Kozin, *Proceedings of the First Symposium on Engineering Applications of Random Function Theory and Probability*, John Wiley & Sons, New York

Kapitaniak, T., Kocarev, L.J. and Chua, L.O. (1993), "Controlling chaos without feedback and control signals", *Int. J. Bifurcat. Chaos*, **3**, 459-468. https://doi.org/10.1142/S0218127493000362.

Kickert, W.J.M. and Mamdani, E.H. (1978), "Analysis of a fuzzy logic controller", *Fuzzy Sets Syst.*, **1**(1), 29-44. https://doi.org/10.1016/B978-1-4832-1450-4.50033-X.

Kim, H. and Adeli, H. (2004), "Hybrid feedback-least mean square algorithm for structural control", *J. Struct. Eng.*, ASCE, **130**(2), 120-127. https://doi.org/10.1061/(ASCE)0733-9445(2004)130:1(120).

Lu, L.T., Chiang, W.L. and Tang, J.P. (1998), "LQG/LTR control methodology in active structure control", *J. Eng. Mech.*, ASCE, **124**(4), 446-454. https://doi.org/10.1061/(ASCE)0733-9399(1998)124:4(446).

Maciejowski, J.M. (1989), *Multivariable Feedback Design*, Addition-Wesley Publishing Co., Chapter 5, 222-264.

Moore, B.C. (1981), "Principal component analysis in linear systems: controllability, observability, and model reduction", *IEEE Tran. Auto. Control*, **26**, 17-31. https://doi.org/10.1109/TAC.1981.1102568.

Mossaheb, S. (1983), "Application of a method of averaging to the study of dithers in nonlinear systems", *Int. J. Control*, **38**, 557-576. https://doi.org/10.1080/00207178308933094.

Stein, G. and Athans, M. (1987), "The LQG/LTR procedure for multivariable feedback control design", *IEEE Tran. Auto. Control*, **32**(2), 105-114. https://doi.org/10.1109/TAC.1987.1104550.

Steinberg, A.M. and Kadushin, I. (1973), "Stabilization of nonlinear systems with dither control", *J. Math. Anal. Appl.*, **43**, 273-284. https://doi.org/10.1016/0022-247X(73)90275-8.

Takagi, T. and Sugeno, M. (1985), "Fuzzy identification of systems and its applications to modeling and control", *IEEE Trans. Syst., Man, Cybern.*, **1**, 116-132. https://doi.org/10.1109/TSMC.1985.6313399.

Tsai, P.W., Pan, J.S., Liao, B.Y., Tsai, M.J. and Istanda, V. (2012), "Bat algorithm inspired algorithm for solving numerical optimization problems", *Appl. Mech. Mater.*, **148**, 134-137. https://doi.org/10.4028/www.scientific.net/AMM.148-149.134.

Wang, H.O. and Abed, E.H. (1995), "Bifurcation control of a chaotic system", *Automatica*, **31**, 1213-1226. https://doi.org/10.1016/0005-1098(94)00146-A.

Wang, H.O. and Tanaka, K. (1996), "An LMI-based stable fuzzy control of nonlinear systems and its application to control of chaos", *IEEE Int. Conf. on Fuzzy Systems*, 1433-1438. https://doi.org/10.1109/FUZZY.1996.552386.

Wang, H.O., Tanaka, K. and Griffin, M.F. (1996), "An approach to fuzzy control of nonlinear systems: stability and design issues", *IEEE Tran. Fuzzy Syst.*, **4**, 14-23. https://doi.org/10.1109/91.481841.

Yang, J.N., Wu, J.C., Samali, B. and Agrawal, A.K. (1998), "A benchmark problem for response control of wind-excited tall buildings", *Proc. 2nd world Conference on Structural Control*, **2**, John Wiley & Sons, New York.

Zadeh, L.A. (1965), "Fuzzy sets", *Inform. Control*, **8**(3), 338-353. https://doi.org/10.1016/S0019-9958(65)90241-X.

Zames, G. and Shneydor, N.A. (1976), "Dither in nonlinear systems", *IEEE Tran. Automat. Cortrol*, **21**, 660-667. https://doi.org/10.1109/TAC.1976.1101357.

Zames, G. and Shneydor, N.A. (1977), "Structural stabilization on quenching by dither in nonlinear systems", *IEEE Tran. Automat. Contr.*, **22**, 353-361. https://doi.org/10.1109/TAC.1977.1101504.

AT